Modeling soluble surfactants in two-phase flows

By S. S. Jain

1. Motivation and objectives

Surfactants modulate surface tension properties and generate Marangoni forces, and as such, they find diverse applications in multiphase flows across various industries. In the oil and gas sector, they are used for stabilizing emulsions for efficient pipeline transport and to aid in breaking them during oil separation. Chemical-enhanced oil recovery utilizes surfactants to alter interfacial tension, improving oil displacement from reservoirs (Massarweh & Abushaikha 2020). In pharmaceuticals and agrochemicals, surfactants create stable microemulsions to enhance solubility (Castro *et al.* 2014). Environmental applications involve surfactants in bioremediation, aiding contaminant removal (Churchill *et al.* 1995). Surfactants play crucial roles in personal care product formulation (Rhein *et al.* 2006), food industry emulsion stability (Kralova & Sjöblom 2009), and drug delivery systems (Lawrence 1994). They also contribute to enhanced gas-liquid mass transfer in bioprocess engineering and microfluidic manipulation for lab-on-a-chip applications (Baret 2012), showcasing their versatility in optimizing multiphase flow processes.

The effect of surfactants has been studied extensively using various approaches, including theoretical, semi-analytical, and computational techniques, such as boundary integral-based methods as well as sharp-interface- and diffuse-interface-based continuum approaches.

Some of the recent advancements in modeling insoluble surfactants include the volume-of-fluid (VOF)-based formulation presented by James & Lowengrub (2004), finite-element-based methods by Venkatesan *et al.* (2019) and Frachon & Zahedi (2023), segment projection method by Khatri & Tornberg (2011), level-set method by Xu *et al.* (2012), front-tracking method with adaptive mesh refinement by de Jesus *et al.* (2015), immersed-boundary method by Lai *et al.* (2008), hybrid methods by Cui (2011), Cahn-Hilliard-based diffuse interface methods by Abels *et al.* (2019); Di Primio *et al.* (2022); Teigen *et al.* (2009, 2011); Garcke *et al.* (2014) and Ray *et al.* (2021), and second-order phase-field-based method by Jain (2023).

Similarly, soluble surfactants have been modeled extensively, e.g., using finite-element-based formulation with a coupled arbitrary Lagrangian-Eulerian and Lagrangian approach for modeling interfaces by Ganesan & Tobiska (2012), a parametric finite-element approximation for interface and surface finite-element approximation for surfactants by Barrett *et al.* (2015), a segment projection method by Khatri & Tornberg (2014), a level-set method by Xu *et al.* (2018), a front-tracking method by Muradoglu & Tryggvason (2008), an immersed-boundary method by Chen & Lai (2014), Cahn-Hilliard-based diffuse-interface methods by Teigen *et al.* (2009, 2011), and lattice-Boltzmann methods by Liu & Zhang (2010) and Kothari & Komrakova (2023). Other advancements in modeling soluble surfactants include a multiscale modeling approach presented by Booty & Siegel (2010), porous media flows by Zhang *et al.* (2021), and linear stability analysis of effect of soluble surfactants on two-phase flows by Herrada *et al.* (2022). However, to the best of our knowledge, there is no model for transport of soluble surfactants for second-order phase-field methods.

We recently developed a model for transport of interface-confined scalars and insoluble surfactants (Jain 2023) and used it with the accurate conservative diffuse-interface (ACDI) method, a second-order phase-field method. However, this model is not limited to a diffuse-interface approach; it and can be used with any other interface-capturing method. A recent use of this model along with a geometric VOF method is presented by Farsoiya *et al.* (2023). The primary objective of the present work is to extend the previous work by Jain (2023) for modeling transport of soluble surfactants by coupling it with the transport model for scalars in the bulk of one of the phases (Jain & Mani 2023), by modeling adsorption and desorption of the surfactants at the interface. We prove and show that the total concentration of the surfactant remains positive and conserved, which is a physical-realizability condition, using second-order central-difference schemes.

We use a second-order phase-field method, particularly the ACDI method by Jain (2022), to model the interface in a two-phase flow. The proposed model can also be used with a conservative phase-field/diffuse-interface method (Chiu & Lin 2011), a conservative level-set method (Olsson & Kreiss 2005), an accurate conservative level-set method (Desjardins *et al.* 2008), including compressible diffuse-interface methods (Jain *et al.* 2020, 2023), and any other method that results in a hyperbolic tangent interface shape in equilibrium, and when the volume fraction ϕ is bounded between 0 and 1. For coupling with other models, like a Cahn-Hilliard model where the volume fraction takes values between -1 and 1, the proposed model can be affine transformed with respect to the order parameter, such that the change in the range from $[0, 1]$ to the range of values of ϕ that the interface-capturing model admits is accounted for.

2. Phase-field model

In this work, we use the ACDI by Jain (2022), which is an Allen-Cahn-based second-order phase-field model given by

$$\frac{\partial \phi}{\partial t} + \vec{\nabla} \cdot (\vec{u}\phi) = \vec{\nabla} \cdot \left\{ \Gamma \left\{ \epsilon \vec{\nabla}\phi - \frac{1}{4}\left[1 - \tanh^2\left(\frac{\psi}{2\epsilon}\right)\right] \frac{\vec{\nabla}\psi}{|\vec{\nabla}\psi|} \right\} \right\}, \tag{2.1}$$

where ϕ is the phase-field variable that represents the volume fraction, $\vec{u}$ is the velocity, Γ represents the velocity-scale parameter, ϵ is the interface-thickness-scale parameter, and ψ is an auxiliary signed-distance-like variable given by

$$\psi = \epsilon \ln\left(\frac{\phi + \varepsilon}{1 - \phi + \varepsilon}\right), \tag{2.2}$$

where $\varepsilon = 10^{-100}$ is a small number. The parameters are chosen to be $\Gamma \geq |\vec{u}|_{max}$ and $\epsilon > 0.5\Delta x$, and Δt satisfies the explicit Courant-Friedrichs-Lewy criterion, to maintain the boundedness of ϕ (Jain 2022). The ACDI model is more accurate than other phase-field models because it maintains a sharper interface (with only one-to-two grid points across the interface) while being robust and conservative, without the need for any geometric treatment. It has recently been extended to an unstructured framework for simulations in complex geometries (Hwang & Jain 2023) and other multiphysics applications, such as modeling solidification (Brown *et al.* 2023) and boiling (Scapin *et al.* 2022) in two-phase flows. Hence, the ACDI method is chosen as the interface-capturing method in this work.

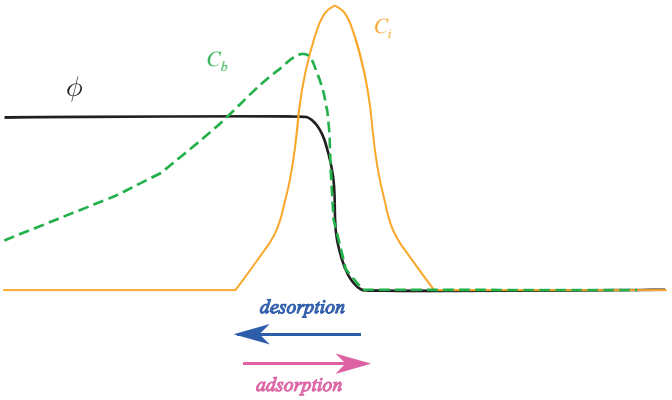

FIGURE 1. Schematic representing the interfacial surfactant concentration, c_i, the bulk surfactant concentration, c_b, and the exchange between these two due to adsorption and desorption of the surfactant. Here, the surfactant is only dissolvable in the bulk of the phase represented by $\phi = 1$.

3. Proposed model for the transport of soluble surfactants in two-phase flows

Surfactants can be modeled using two transport equations (a two-equation model), one for the transport of interfacial surfactant concentration, c_i, and another for the bulk surfactant concentration, c_b, along with source/sink terms for the exchange between these two equations. Both c_i and c_b are volumetric quantities, which represent concentration as the amount of species per unit volume. Accordingly, $\tilde{c}_b = c_b/\phi$ is the local bulk concentration of surfactant defined as the amount of species per unit volume of the phase ϕ, and $\hat{c}_i = c_i/\delta_s$ is the local interfacial concentration of surfactant defined as the amount of species per unit interfacial area, where $\delta_s = |\vec{\nabla}\phi|$ is the surface delta function.

The proposed model for the transport of soluble surfactants in two-phase flows is

$$\frac{\partial c_i}{\partial t} + \vec{\nabla}\cdot(\vec{u}c_i) = \vec{\nabla}\cdot\left[D_i\left\{\vec{\nabla}c_i - \frac{2(0.5-\phi)\vec{n}c_i}{\epsilon}\right\}\right] + \hat{j}\delta_s, \tag{3.1}$$

$$\frac{\partial c_b}{\partial t} + \vec{\nabla}\cdot(\vec{u}c_b) = \vec{\nabla}\cdot\left[D_b\left\{\vec{\nabla}c_b - \frac{(1-\phi)\vec{n}c_b}{\epsilon}\right\}\right] - \hat{j}\delta_s, \tag{3.2}$$

where $\hat{j} = r_a\tilde{c}_b(\hat{c}_{i,\infty} - \hat{c}_i) - r_d\hat{c}_i$ is the source/sink term that arises due to species adsorption into and desorption out of the interface (Martínez-Vitela & Gracia-Fadrique 2020) (Figure 1). Surfactant may saturate when $\hat{c}_i$ reaches $\hat{c}_{i,\infty}$. Here, r_a is the rate of adsorption of surfactant from the bulk into the surface and r_d is the rate of desorption of surfactant from the surface to the bulk; D_i and D_b are the interfacial and bulk diffusivity of the surfactant, respectively; and $\vec{n} = \vec{\nabla}\phi/|\vec{\nabla}\phi| = \vec{\nabla}\psi/|\vec{\nabla}\psi|$ is the interface normal vector.

The second term on the right-hand side of Eqs. (3.1) and (3.2) are artificial sharpening terms. The effect of these sharpening fluxes is to prevent the diffusion of interfacial surfactant on both sides of the interface, to confine it to the interface region, and to prevent the diffusion of bulk surfactant into the other phase, as shown in Figure 1. Additional consistent terms and alternate model forms can be derived (Appendix A) for the proposed model; however, these terms are in non-conservative form and could also make the model non-robust due to the need for division by ϕ and δ_s. Therefore, they are less preferred.

3.1. *Two-way coupling*

To account for two-way coupling with hydrodynamics, this work uses a linearized version of the Langmuir equation of state (EOS), which relates the surfactant concentration to the surface tension coefficient. The Langmuir EOS (Tricot 1997) can be written as

$$\sigma(\hat{c}_i) = \sigma_0 \left[1 + \frac{RT\hat{c}_{i,\infty}}{\sigma_0} \ln\left(1 - \frac{\hat{c}}{\hat{c}_{i,\infty}} \right) \right], \tag{3.3}$$

where R is the ideal gas constant, T is the absolute temperature, $\hat{c}_{i,\infty}$ is the maximum interfacial surfactant concentration, and σ_0 is the surface tension for the clean interface. In the low surfactant concentration limit, this can be reduced to a linear model (also called Henry's EOS) as

$$\sigma(\hat{c}_i) = \sigma_0 \left(1 - Ma \frac{\hat{c}}{\hat{c}_{i,\infty}} \right), \tag{3.4}$$

where $Ma = RT\hat{c}_{i,\infty}/\sigma_0$ is the Marangoni elasticity number, which is a measure of sensitivity of the surface tension to the surfactant concentration.

With a varying surface tension coefficient, the surface tension force can be modeled as (Landau & Lifshitz 2013)

$$\vec{F}_\sigma = \sigma\kappa\vec{\nabla}\phi - (\vec{\nabla}\sigma)|\vec{\nabla}\phi|, \tag{3.5}$$

where the first term is the capillary force and the second term is the Marangoni force.

4. Positivity

In the absence of exchange of the surfactant between the bulk and the interface, Eq. (3.1) reduces to a transport model for an interface-confined scalar (Jain 2023), and Eq. (3.2) reduces to a transport model for an immiscible scalar (Jain & Mani 2023). In these settings, c_i and c_b remain positive if

$$\Delta x \leq \left(\frac{2D}{|u|_{\max} + \frac{D}{\epsilon}} \right) \tag{4.1}$$

and

$$\Delta t \leq \frac{\Delta x^2}{2N_d D} \tag{4.2}$$

are satisfied, where D is D_i for c_i and D_b for c_b, Δx is the grid-cell size, Δt is the time-step size, $|u|_{\max}$ is the maximum fluid velocity in the domain, and N_d is the number of dimensions. Note that this also requires ϕ_i^k to be bounded between 0 and 1, $\forall k \in \mathbb{Z}^+$ and $\forall i$, which is guaranteed to be satisfied with the ACDI method (Jain 2022). If $\epsilon = \Delta x$, then the constraint in Eq. (4.1) reduces to

$$\Delta x \leq \frac{D}{|u|_{\max}} \text{ or } Pe_c \leq 1, \tag{4.3}$$

where $Pe_c = \Delta x|u|_{\max}/D$ is the cell Péclet number.

Note that, when we sum up Eqs. (3.1) and (3.2), we obtain a transport equation for total surfactant concentration $c_i + c_b$, where the source/sink terms in these equations cancel out exactly. Therefore, it is easy to see that the conditions in Eqs. (4.1) or (4.3) and (4.2) are sufficient to maintain the positivity of the total surfactant concentration field.

5. Numerical methods

In this work, we use a second-order central scheme for spatial discretization and a fourth-order Runge-Kutta scheme for time stepping for the proposed model in Section 3. A skew-symmetric-like flux-splitting approach (Jain & Moin 2022) is adopted for the discretization of the ACDI method in Eq. (2.1).

6. Simulation results

In this section, the proposed model for soluble surfactant is used to simulate of surfactant adsorbing onto a droplet interface, and the model is verified against the analytical solution in this simplified setting. The positivity of the surfactant was preserved in this simulation. A two-way coupled simulation of effect of surfactants on droplet oscillation is also presented.

6.1. *Surfactant adsorption*

This canonical case was previously used by Teigen *et al.* (2009) and Muradoglu & Tryggvason (2008) as a verification test. Initially, a clean droplet of radius 1 is placed at the center of a domain of size 4×4 [Figure 2(a)], discretized into a grid of size 100×100. The bulk phase has a uniform initial surfactant concentration of 1 (Figure 2(b)). A simplified adsorption isotherm

$$\hat{j} = r_a \tilde{c}_b$$

with $r_a = 1$ is used in this case. The surfactant adsorbs onto the interface, the interfacial concentration increases with time, and the bulk concentration reduces close to the interface due to the adsorption. The interfacial and bulk surfactant concentration are shown in Figure 2(c,d) at time $t = 0.1$.

The evolution of bulk surfactant concentration is governed by a heat equation with a sink at the interface location, and it was solved by Teigen *et al.* (2009) using a higher-order scheme to obtain a semi-analytical reference solution. We use this reference solution to compare against the accuracy of the proposed model in this work. Figure 3 shows the local bulk concentration outside the drop at various times and compares it with the semi-analytical reference solution from Teigen *et al.* (2009). The present method compares well with the reference solution, verifying the method.

6.2. *Droplet oscillation with surfactants*

In this section, we present a simulation of effect of surfactant on an oscillating droplet in a domain of size 1×1. A initially clean ellipse-shaped droplet with semi-major and semi-minor axes of sizes 0.2 and 0.1, respectively, is placed in the center of the domain. The bulk phase has a uniform initial surfactant concentration of 1. Three simulations are performed, one (a) without surfactant (clean case), and two cases with surfactant with (b) $r_d = 1$ and (c) $r_d = 0.5$. Other parameters are chosen to be $\sigma_0 = 1$, $r_a = 1$, $Ma = 1$, and $\hat{c}_{i,\infty} = 1$.

Figure 4 shows the kinetic energy in the domain as a function of time. Due to the exchange of energy between kinetic energy and surface energy, this plot is a signature of droplet oscillation. In the clean case, the droplet oscillates at its natural frequency throughout the simulation, as expected. But with surfactants, the frequency of oscillation is modified and the droplet oscillation is damped more quickly. For both cases with $r_d = 1, 0.5$, the droplet behavior is similar up to $t \approx 1$ because of the same r_a values. But beyond $t \approx 1$, the case with $r_d = 0.5$ has higher kinetic energy, probably because

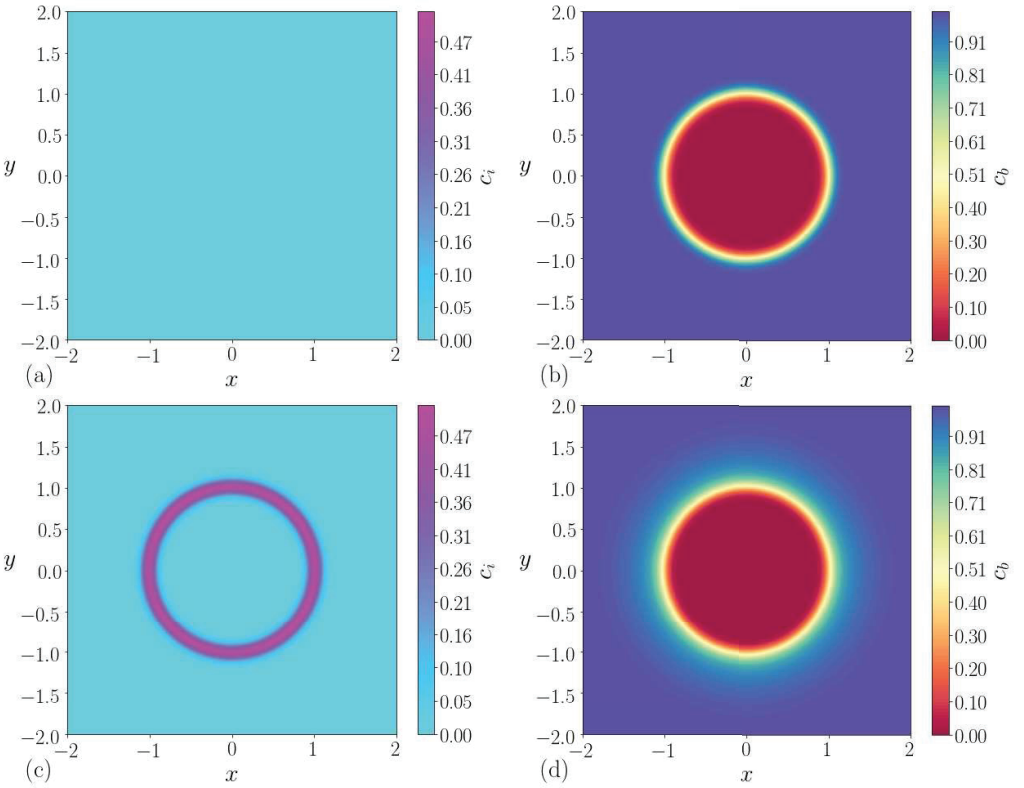

FIGURE 2. (a,b) Initial interfacial and bulk surfactant concentrations, respectively, and (c,d) interfacial and bulk surfactant concentrations at time $t = 0.1$.

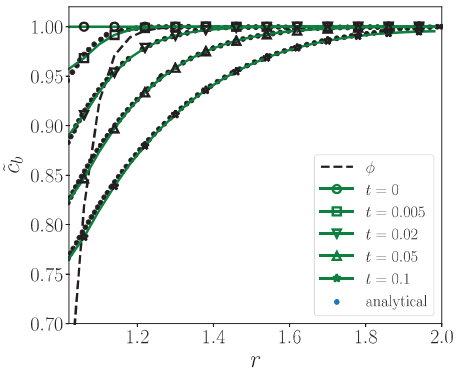

FIGURE 3. Local bulk concentration outside the drop at various times.

of lower surface energy contribution (because of reduced surface tension due to a higher interfacial surfactant concentration).

The damping of the oscillations of the droplet due to surfactant can be explained by looking at the distribution of surfactant on the interface. Figure 5 shows the interfacial and bulk concentrations at two time instances, $t = 0.325$ and $t = 0.675$. Figure 5(a) shows higher concentration of interfacial surfactant on the west and east poles of the

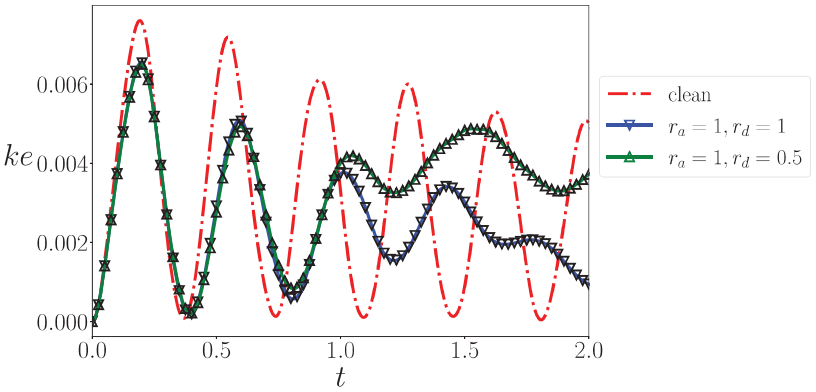

FIGURE 4. Kinetic energy of droplet oscillation with and without surfactants.

drop. This is because the droplet is undergoing compression along the horizontal axis. But this distribution of surfactant concentration will result in a Marangoni force in the opposite direction which opposes this droplet deformation. Similarly, in Figure 5(c), the droplet compression along the vertical axis is being opposed by the Marangoni forces in the opposite direction due to higher surfactant concentrations at the north and south poles of the drop. These simulations illustrate the effect of soluble surfactants on the droplet dynamics.

7. Conclusion

In this work, a model for the transport of soluble surfactants in two-phase flows is developed. The model is solved with a second-order phase-field model; however, it also can be used with other interface-capturing methods. The model discretely conserves the total surfactant mass and results in positive surfactant concentrations, a physical-realizability condition, provided the given positivity criterion is satisfied.

The proposed model was used to simulate adsorption of surfactant onto a droplet and to study its effect on the droplet dynamics in a two-dimensional setting. The model was verified to maintain the positivity of the surfactant concentration, and the accuracy of the model was verified by comparing it with analytical solutions for the adsorption process.

Acknowledgments

S. S. J. acknowledges financial support from Boeing Co.

Appendix A: Alternate models

Following the procedure used by Jain *et al.* (2020), additional consistent terms can be derived for the proposed model as

Model A:

$$\frac{\partial c_s}{\partial t} + \vec{\nabla}\cdot(\vec{u}c_s) = \vec{\nabla}\cdot\left[D\left\{\vec{\nabla}c_s - \frac{2(0.5-\phi)\vec{n}c_s}{\epsilon}\right\}\right] + \vec{n}\cdot\vec{\nabla}\left(\vec{\nabla}\cdot\vec{a}\right)\hat{c}_s + \hat{j}\delta_s, \tag{7.1}$$

$$\frac{\partial c_b}{\partial t} + \vec{\nabla}\cdot(\vec{u}c_b) = \vec{\nabla}\cdot\left[D\left\{\vec{\nabla}c_b - \frac{(1-\phi)\vec{n}c_b}{\epsilon}\right\}\right] + \vec{\nabla}\cdot(\tilde{c}_b\vec{a}) - \hat{j}\delta_s. \tag{7.2}$$

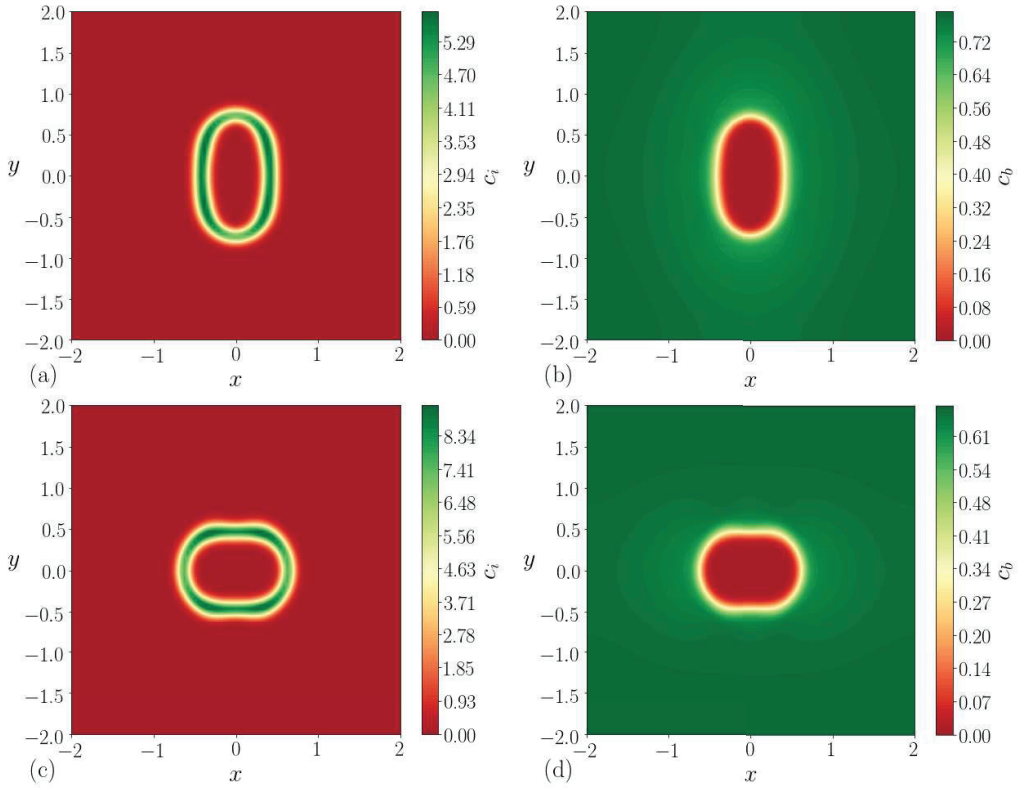

FIGURE 5. (a,b) Interfacial and bulk surfactant concentrations, respectively, at time $t = 0.325$ and (c,d) interfacial and bulk surfactant concentrations at time $t = 0.675$.

However, note that the additional consistent terms are in a non-conservative form; therefore, care must be taken in using this model form. Using a model form based on Teigen *et al.* (2009), we can also write the proposed model as

Model B:

$$\frac{\partial c_s}{\partial t} + \vec{\nabla} \cdot (\vec{u} c_s) = \vec{\nabla} \cdot \left(D \delta_s \vec{\nabla} \hat{c}_s \right) + \vec{n} \cdot \vec{\nabla} \left(\vec{\nabla} \cdot \vec{a} \right) \hat{c}_s + \hat{j} \delta_s, \tag{7.3}$$

$$\frac{\partial c_b}{\partial t} + \vec{\nabla} \cdot (\vec{u} c_b) = \vec{\nabla} \cdot \left(D \phi \vec{\nabla} \tilde{c}_b \right) + \vec{\nabla} \cdot (\tilde{c}_b \vec{a}) - \hat{j} \delta_s. \tag{7.4}$$

The additional terms in Eqs. (7.2) and (7.4) are the same as the ones introduced by Jain *et al.* (2020). The advantage of **Model B** is that it does not assume a perfect equilibrium interface; however, it requires computation of $\hat{c}_s$ in the diffusion term, which requires division by δ_s and could be non-robust.

REFERENCES

ABELS, H., GARCKE, H. & WEBER, J. 2019 Existence of weak solutions for a diffuse interface model for two-phase flow with surfactants. *Commun. Pure Appl. Anal.* **18**, 195–225.

BARET, J.-C. 2012 Surfactants in droplet-based microfluidics. *Lab Chip* **12**, 422–433.

Barrett, J. W., Garcke, H. & Nürnberg, R. 2015 Stable finite element approximations of two-phase flow with soluble surfactant. *J. Comput. Phys.* **297**, 530–564.

Booty, M. & Siegel, M. 2010 A hybrid numerical method for interfacial fluid flow with soluble surfactant. *J. Comput. Phys.* **229**, 3864–3883.

Brown, L., Jain, S. & Moin, P. 2023 A phase field model for simulating the freezing of supercooled liquid droplets. Tech. Pap. 2023-01-1454. SAE.

Castro, M. J., Ojeda, C. & Cirelli, A. F. 2014 Advances in surfactants for agrochemicals. *Environ. Chem. Lett.* **12**, 85–95.

Chen, K.-Y. & Lai, M.-C. 2014 A conservative scheme for solving coupled surface-bulk convection–diffusion equations with an application to interfacial flows with soluble surfactant. *J. Comput. Phys.* **257**, 1–18.

Chiu, P.-H. & Lin, Y.-T. 2011 A conservative phase field method for solving incompressible two-phase flows. *J. Comput. Phys.* **230** (1), 185–204.

Churchill, P. F., Dudley, R. J. & Churchill, S. A. 1995 Surfactant-enhanced bioremediation. *Waste Manage.* **15**, 371–377.

Cui, Y. 2011 *A computational fluid dynamics study of two-phase flows in the presence of surfactants*. PhD Thesis, Univ. N. H.

Desjardins, O., Moureau, V. & Pitsch, H. 2008 An accurate conservative level set/ghost fluid method for simulating turbulent atomization. *J. Comput. Phys.* **227**, 8395–8416.

Di Primio, A., Grasselli, M. & Wu, H. 2022 Well-posedness for a Navier-Stokes-Cahn-Hilliard system for incompressible two-phase flows with surfactant. *arXiv Preprint* arXiv:2201.09022.

Farsoiya, P. K., Popinet, S., Stone, H. & Deike, L. 2023 Direct numerical simulations of surfactant transport and Marangoni forces at the interface between two fluids. *Bulletin of the American Physical Society* .

Frachon, T. & Zahedi, S. 2023 A cut finite element method for two-phase flows with insoluble surfactants. *J. Comput. Phys.* **473**, 111734.

Ganesan, S. & Tobiska, L. 2012 Arbitrary Lagrangian–Eulerian finite-element method for computation of two-phase flows with soluble surfactants. *J. Comput. Phys.* **231**, 3685–3702.

Garcke, H., Lam, K. F. & Stinner, B. 2014 Diffuse interface modelling of soluble surfactants in two-phase flow. *Commun. Math. Sci.* **12**, 1475–1522.

Herrada, M., Ponce-Torres, A., Kaneelil, P., Pahlavan, A., Stone, H. & Montanero, J. 2022 Effect of a soluble surfactant on the linear stability of two-phase flows in a finite-length channel. *Phys. Rev. Fluids* **7**, 114003.

Hwang, H. & Jain, S. S. 2023 A robust phase-field method for two-phase flows on unstructured grids. *arXiv Preprint* arXiv:2310.10795 .

Jain, S. S. 2022 Accurate conservative phase-field method for simulation of two-phase flows. *J. Comput. Phys.* **469**, 111529.

Jain, S. S. 2023 A model for transport of interface-confined scalars and insoluble surfactants in two-phase flows. *arXiv preprint arXiv:2311.11076* .

Jain, S. S., Adler, M. C., West, J. R., Mani, A., Moin, P. & Lele, S. K. 2023 Assessment of diffuse-interface methods for compressible multiphase fluid flows and elastic-plastic deformation in solids. *J. Comput. Phys.* **475**, 111866.

Jain, S. S. & Mani, A. 2023 A computational model for transport of immiscible scalars in two-phase flows. *J. Comput. Phys.* **475**, 111843.

Jain, S. S., Mani, A. & Moin, P. 2020 A conservative diffuse-interface method for compressible two-phase flows. *J. Comput. Phys.* **418**, 109606.

Jain, S. S. & Moin, P. 2022 A kinetic energy–and entropy-preserving scheme for compressible two-phase flows. *J. Comput. Phys.* **464**, 111307.

James, A. J. & Lowengrub, J. 2004 A surfactant-conserving volume-of-fluid method for interfacial flows with insoluble surfactant. *J. Comput. Phys.* **201**, 685–722.

de Jesus, W. C., Roma, A. M., Pivello, M. R., Villar, M. M. & da Silveira-Neto, A. 2015 A 3D front-tracking approach for simulation of a two-phase fluid with insoluble surfactant. *J. Comput. Phys.* **281**, 403–420.

Khatri, S. & Tornberg, A.-K. 2011 A numerical method for two phase flows with insoluble surfactants. *Comput. Fluids* **49**, 150–165.

Khatri, S. & Tornberg, A.-K. 2014 An embedded boundary method for soluble surfactants with interface tracking for two-phase flows. *J. Comput. Phys.* **256**, 768–790.

Kothari, Y. & Komrakova, A. 2023 Free-energy-based lattice Boltzmann model for emulsions with soluble surfactant. *Chem. Eng. Sci.* **285**, 119609.

Kralova, I. & Sjöblom, J. 2009 Surfactants used in food industry: a review. *J. Disper. Sci. Technol.* **30**, 1363–1383.

Lai, M.-C., Tseng, Y.-H. & Huang, H. 2008 An immersed boundary method for interfacial flows with insoluble surfactant. *J. Comput. Phys.* **227**, 7279–7293.

Landau, L. D. & Lifshitz, E. M. 2013 *Course of Theoretical Physics.*, Vol. 6. Elsevier.

Lawrence, M. J. 1994 Surfactant systems: their use in drug delivery. *Chem. Soc. Rev.* **23**, 417–424.

Liu, H. & Zhang, Y. 2010 Phase-field modeling droplet dynamics with soluble surfactants. *J. Comput. Phys.* **229**, 9166–9187.

Martínez-Vitela, M. A. & Gracia-Fadrique, J. 2020 The Langmuir-Gibbs surface equation of state. *Fluid Phase Equilibria* **506**, 112372.

Massarweh, O. & Abushaikha, A. S. 2020 The use of surfactants in enhanced oil recovery: A review of recent advances. *Energy Reports* **6**, 3150–3178.

Muradoglu, M. & Tryggvason, G. 2008 A front-tracking method for computation of interfacial flows with soluble surfactants. *J. Comput. Phys.* **227**, 2238–2262.

Olsson, E. & Kreiss, G. 2005 A conservative level set method for two phase flow. *J. Comput. Phys.* **210**, 225–246.

Ray, D., Liu, C. & Riviere, B. 2021 A discontinuous Galerkin method for a diffuse-interface model of immiscible two-phase flows with soluble surfactant. *Computat. Geosci.* **25**, 1775–1792.

Rhein, L. D., Schlossman, M., O'Lenick, A. & Somasundaran, P. 2006 *Surfactants in Personal Care Products and Decorative Cosmetics*. CRC Press.

Scapin, N., Shahmardi, A., Chan, W., Jain, S., Mirjalili, S., Pelanti, M. & Brandt, L. 2022 A mass-conserving pressure-based method for two-phase flows with phase change. *Proceedings of the Summer Program*, Center for Turbulence Research, Stanford University, pp. 195–204.

Teigen, K. E., Li, X., Lowengrub, J., Wang, F. & Voigt, A. 2009 A diffuse-interface approach for modeling transport, diffusion and adsorption/desorption of material quantities on a deformable interface. *Commun. Math. Sci.* **4**, 1009–1037.

Teigen, K. E., Song, P., Lowengrub, J. & Voigt, A. 2011 A diffuse-interface

method for two-phase flows with soluble surfactants. *J. Comput. Phys.* **230**, 375–393.

Tricot, Y.-M. 1997 Surfactants: static and dynamic surface tension. In *Liquid Film Coating: Scientific Principles and Their Technological Implications*, pp. 99–136. Springer.

Venkatesan, J., Padmanabhan, A. & Ganesan, S. 2019 Simulation of viscoelastic two-phase flows with insoluble surfactants. *J. Non-Newton. Fluid* **267**, 61–77.

Xu, J.-J., Shi, W. & Lai, M.-C. 2018 A level-set method for two-phase flows with soluble surfactant. *J. Comput. Phys.* **353**, 336–355.

Xu, J.-J., Yang, Y. & Lowengrub, J. 2012 A level-set continuum method for two-phase flows with insoluble surfactant. *J. Comput. Phys.* **231**, 5897–5909.

Zhang, J., Liu, H., Wei, B., Hou, J. & Jiang, F. 2021 Pore-scale modeling of two-phase flows with soluble surfactants in porous media. *Energ. Fuel.* **35**, 19374–19388.